OXFORD UNIVERSITY PRESS | Brain

Stage-specific associations between plasma neurofilament light and imaging biomarkers of Alzheimer's disease

Journal:	*Brain*
Manuscript ID	BRAIN-2020-01201.R1
Manuscript Type:	Original Article
Date Submitted by the Author:	28-Jul-2020
Complete List of Authors:	Benedet, Andrea; McGill University, Translational Neuroimaging Laboratory, The McGill University Research Centre for Studies in Aging Leuzy, Antoine; Lund University, Clinical Sciences, Malmö Pascoal, Tharick; McGill University, Translational Neuroimaging Laboratory, The McGill University Research Centre for Studies in Aging Ashton, Nicholas; University of Gothenburg, Neuroscience and Physiology Mathotaarachchi, Sulantha; McGill University Savard, Mélissa; McGill University, McGill University Research Centre for Studies in Aging Therriault, Joseph; McGill University, Integrated Program in Neuroscience Kang, Min Su; McGill University, Translational Neuroimaging Laboratory, The McGill University Research Centre for Studies in Aging Chamoun, Mira; McGill University, Translational Neuroimaging Laboratory, The McGill University Research Centre for Studies in Aging Schöll, Michael; University of Gothenburg, Psychiatry and Neurochemistry R. Zimmer, Eduardo; Federal University of Rio Grande do Sul Gauthier, Serge; McGill University, The McGill University Research Centre for Studies in Aging Labbe, Aurelie; HEC Montreal Zetterberg, Henrik; University of Gothenburg, Psychiatry and Neurochemistry Rosa-Neto, Pedro; McGill University, Translational Neuroimaging Laboratory, The McGill University Research Centre for Studies in Aging Blennow, Kaj; University of Gothenburg Sahlgrenska Academy, Institute of Neuroscience and Physiology, Department of Psychiatry and Neurochemistry; Sahlgrenska University Hospital, Clinical Neurochemistry Laboratory
Subject category:	Dementia
To search keyword list, use whole or part words followed by an *:	Alzheimer's disease < DEMENTIA, Amyloid imaging < DEMENTIA, Brain atrophy < DEMENTIA, Dementia: biomarkers < DEMENTIA, Tau imaging < DEMENTIA, Neurodegeneration: biomarkers < NEURODEGENERATION: CELLULAR AND MOLECULAR, Neurofilaments < NEURODEGENERATION: CELLULAR AND MOLECULAR

Stage-specific links between plasma neurofilament light and imaging biomarkers of Alzheimer's disease

Andréa L. Benedet PhD[1,2,*], Antoine Leuzy PhD[3,*], Tharick A. Pascoal MD PhD[1], Nicholas J. Ashton PhD[4,5,6,7], Sulantha Mathotaarachchi MSc[1], Melissa Savard MSc[1], Joseph Therriault BSc[1], Min Su Kang BSc[1], Mira Chamoun PhD[1], Michael Schöll PhD[3,4,5,8], Eduardo R. Zimmer PhD[9,10], Prof Serge Gauthier MD FRCPC[9], Aurélie Labbe PhD[11], Prof Henrik Zetterberg MD PhD[4,8,12,13], Prof Pedro Rosa-Neto MD PhD[1,14,15] and Prof Kaj Blennow MD PhD[4,12,★] for the Alzheimer's Disease Neuroimaging Initiative[+]

[1]Translational Neuroimaging Laboratory, McGill Centre for Studies in Aging, McGill University, Montreal, QC, Canada; [2]CAPES Foundation, Ministry of Education of Brazil, Brasília, Brazil; [3]Clinical Memory Research Unit, Department of Clinical Sciences, Malmö, Lund University, Lund, Sweden; [4]Department of Psychiatry and Neurochemistry, Institute of Neuroscience & Physiology, the Sahlgrenska Academy at the University of Gothenburg, Mölndal, Sweden; [5]Wallenberg Centre for Molecular and Translational Medicine, University of Gothenburg, Gothenburg, Sweden; [6]King's College London, Institute of Psychiatry, Psychology & Neuroscience, Maurice Wohl Clinical Neuroscience Institute, London, UK; [7]NIHR Biomedical Research Centre for Mental Health & Biomedical Research Unit for Dementia at South London & Maudsley NHS Foundation, London, UK; [8]Department of Neurodegenerative Disease, UCL Institute of Neurology, London, UK; [9]Alzheimer's Disease Research Unit, The McGill University Research Centre for Studies in Aging, Montreal, McGill University, Montreal, QC, Canada; [10]Departament of Pharmacology, Universidade Federal do Rio Grande do Sul, Porto Alegre, Brazil; [11]Department of Decision Sciences, HEC Montreal, Montreal, QC, Canada;[12]Clinical Neurochemistry Laboratory, Sahlgrenska University Hospital, Mölndal, Sweden; [13]UK Dementia Research Institute at UCL, London, UK; [14]Montreal Neurological Institute, Montreal, QC, Canada; [15]Department of Neurology and Neurosurgery, McGill University, Montreal, QC, Canada

[+]Data used in preparation of this article were also obtained from the Alzheimer's Disease Neuroimaging Initiative (ADNI) database (adni.loni.usc.edu). As such, the investigators within the ADNI contributed

to the design and implementation of ADNI and/or provided data but did not participate in analysis or writing of this report. A complete listing of ADNI investigators can be found at: http://adni.loni.usc.edu/wp-content/uploads/how_to_apply/ADNI_Acknowledgement_List.pdf

*These authors contributed equally to this work.

⋆**Corresponding author:** Kaj Blennow, MD, PhD

Department of Psychiatry and Neurochemistry, Institute of Neuroscience and Physiology

The Sahlgrenska Academy, University of Gothenburg, S-431, 80 Mölndal, Sweden

Tel: +46 (0)31-342 10 00

Email: kaj.blennow@neuro.gu.se

Abstract

Neurofilament light is a marker of neuroaxonal injury, a prominent feature of Alzheimer's disease. It remains uncertain, however, how it relates to amyloid and tau pathology or neurodegeneration across the Alzheimer's disease continuum. The aim of this study was to investigate how plasma neurofilament light relates to amyloid and tau PET and MRI measures of brain atrophy in participants with and without cognitive impairment. We retrospectively examined the association between plasma neurofilament light and MRI measures of gray/white matter volumes in the Alzheimer's Disease Neuroimaging Initiative (ADNI; n=1149, 382 cognitively unimpaired (CU) controls and 767 cognitively impaired (CI) participants [mild cognitive impairment, n=420; Alzheimer's disease dementia, n=347). Longitudinal plasma neurofilament light was measured using Single molecule array technology. Cross-sectional associations between plasma neurofilament light and PET amyloid and tau measures were independently assessed in two cohorts (ADNI, n=198: 110 CU, 88 CI [MCI n=67, Alzheimer's disease dementia n=21; data accessed October 2018]; and TRIAD, n=116: 74 CU, 42 CI [MCI n=16, Alzheimer's disease dementia n=26]; data obtained November 2017-January 2019). Associations between plasma neurofilament light and imaging-derived measures were examined voxel-wise using linear regression (cross-sectional) and linear mixed effect models (longitudinal). Cross-sectional analyses in both cohorts showed that plasma neurofilament light was associated with PET findings in brain regions typically affected by Alzheimer's disease; associations were specific to amyloid PET in CU and tau PET in CI (P<0·05). Longitudinal analyses showed that neurofilament light levels were associated with gray/white matter volume loss; gray matter atrophy in CU was specific to *APOE* ε4 carriers (P<0·05). These findings suggest that plasma neurofilament light increases in response to amyloid-related neuronal injury in preclinical stages of Alzheimer's disease, but is related to tau-mediated

neurodegeneration in symptomatic patients. As such, plasma neurofilament light may a useful measure to monitor effects in disease-modifying drug trials.

Key words: Neurofilament light, amyloid, tau, MRI, Alzheimer's disease.

Introduction

Alzheimer's disease (AD) is biologically characterized by the accumulation of extracellular amyloid-β (Aβ) plaques and intracellular tau aggregates. These pathological hallmarks are thought to result in neurodegenerative changes via direct and synergistic effects, leading, ultimately, to cognitive impairment and functional decline. Increasingly, biomarkers of these biological processes are used in both clinical practice and research settings and in the context of clinical trials and drug development. The most commonly used AD biomarkers include structural magnetic resonance imaging (MRI)-based measures of atrophy, positron emission tomography (PET)-based imaging of brain glucose metabolism, Aβ, and tau tangles, and cerebrospinal fluid (CSF) measures of Aβ, tau and neuronal injury. Hampering the use of these biomarkers, however, is the high cost and limited availability of imaging-based measures, especially PET, and the perceived invasiveness of CSF sampling. As a result, blood-based biomarkers are increasingly seen as simplified initial screening step in primary care (Hampel *et al.*, 2018). One such potential measure is the axonal injury marker neurofilament light (NfL) (Zetterberg, 2016). NfL is a key structural component of the neuronal cytoskeleton and is abundantly expressed in large-caliber myelinated axons (Trojanowski *et al.*, 1986). In response to injury, NfL is released into the CSF and blood; biofluid concentrations of NfL, however, also increase in an age-dependent manner (Bridel *et al.*, 2019). NfL has been shown to be elevated in both plasma (Mattsson *et al.*, 2019) and CSF (Sjogren *et al.*, 2001) in sporadic, familial and preclinical AD (Weston *et al.*, 2017; Preische *et al.*, 2019; Quiroz *et al.*, 2020), and to correlate with cognitive, biochemical, imaging-based measures and *post-mortem* findings in AD (Zetterberg *et al.*, 2016; Mattsson *et al.*, 2017; Ashton *et al.*, 2019; Mattsson *et al.*, 2019). Studies addressing associations between plasma NfL and imaging markers are few (Zetterberg *et al.*, 2016; Mattsson *et al.*, 2017; Chatterjee *et al.*, 2018; Ashton *et al.*, 2019; Benedet *et al.*, 2019; Mattsson *et al.*, 2019; Thijssen *et al.*, 2020), however, and these have

mostly been confined to explore pre-defined regions of interest and a global index of white matter (WM) change.

With consideration for the above, we herein investigated the association between plasma NfL concentrations and cross-sectional Aβ and tau PET as well as longitudinal MRI-derived measures of grey matter (GM) and WM atrophy in a large number of cognitively unimpaired (CU) and cognitively impaired individuals (CI; mild cognitive impairment (MCI) and dementia due to AD). As plasma NfL alterations are not considered specific to a particular disease but are instead linked to neurodegeneration processes, we hypothesized that, across the clinical spectrum of AD, plasma NfL would be differentially related to Aβ and tau pathology. We also hypothesized that plasma NfL would be associated with progressive GM and WM atrophy.

Methods

Study design and participants

This retrospective study was based on data from the ADNI (AD Neuroimaging Initiative; data downloaded October, 2018) and TRIAD (Translational Biomarkers in Aging and Dementia; data collected between November, 2017 and January, 2019) cohorts as described in Fig. 1 (see also appendix, p2, for a detailed description of the cohorts). In ADNI, CU participants had a Mini-Mental State Examination (MMSE) score of 24 or greater and a Clinical Dementia Rating (CDR) score of 0. CI were defined as MCI if they had objective memory loss based on delayed recall performance on the Wechsler Memory Scale (logical memory II; (>1 SD below the mean), MMSE scores ≥ 24, a CDR score of 0·5 and preserved activities of daily living (i.e. no dementia). CI individuals with AD dementia fulfilled the National Institute of Neurological Communicative Disorders and Stroke–Alzheimer Disease and Related Disorders Association (NINCDS-ADRDA) criteria for probable AD (McKhann *et al.*, 1984), had MMSE scores

between 20 and 26, and CDR scores between 0·5 and 1. In TRIAD, CU and CI groups being defined using the same criteria as in ADNI, though AD participants had a CDR between 1 and 2. Exclusion criteria for both cohorts included the presence of medical contraindications and being enrolled in other trials or studies concurrently.

Longitudinal analysis was performed using ADNI data only; cross sectional-analyses were performed in both cohorts, with the TRIAD cohort included to validate ADNI based findings. The same inclusion/exclusion criteria were used to define CU and CI groups in ADNI and TRIAD. For the longitudinal analysis in ADNI, longitudinal plasma NfL (up to 48 months) and MRI-based measures (closest in time to plasma collection) were obtained for 1149 participants (including 382 CU controls and 767 CI participants [MCI, n=420; AD dementia, n=347]), as described below. The cross-sectional (ADNI based) analysis between plasma NfL and PET based measures of Aβ ([^{18}F]florbetapir) and tau ([^{18}F]flortaucipir), was also investigated using a subset of participants (n=198, including 110 CU controls and 88 CI participants [MCI, n=67; AD dementia, n=21]). This cross-sectional analysis was subsequently replicated in 116 participants from the TRIAD cohort (including 74 CU controls and 42 CI participants [MCI, n=16; AD dementia, n=26]) with plasma NfL, Aβ ([^{18}F]AZD4694) and tau ([^{18}F]MK6240) PET. For these ADNI and TRIAD based cross-sectional analyses, selected PET scans were those closest in time to plasma NfL collection.

Regional ethical committees of all participating institutions approved the ADNI study. The Research Ethics Board of the Montreal Neurological Institute as well as the Faculty of Medicine Research Ethics Office, McGill University, approved the TRIAD study. All study participants provided written informed consent.

Plasma quantification

For both cohorts, plasma NfL concentrations were measured using an in-house immunoassay on the Single molecule array (Simoa) HD-1 Analyser (Quanterix, Billerica, MA), as previously described (Gisslen *et al.*, 2016). Measurements were performed using a single batch of reagents for each cohort (for further details, see appendix p3).

Voxel-based morphometry

For ADNI, 1.5T and 3T T1-weighted MRI preprocessed scans were segmented into probabilistic GM and WM maps. These were then non-linearly registered to the ADNI template and smoothed with a Gaussian kernel. For further details pertaining to image pre-processing see the appendix p4.

Brain Aβ and tau imaging

In the ADNI cohort, Aβ-load was estimated using [^{18}F]florbetapir (40-70 min post-injection) standardized uptake value ratios (SUVR) and the cerebellar GM as reference region.

Tau-load was estimated using [^{18}F]flortaucipir (80-100 min post-injection) SUVR, using the inferior cerebellar GM as reference region. Full PET details are described in the appendix, p4.

In TRIAD, Aβ ([^{18}F]AZD4694; 40–70 minutes post-injection) and tau ([^{18}F]MK6240; 90–110 minutes post-injection) PET scans were acquired with a Siemens High Resolution Research Tomograph (Siemens Medical Solutions, Knoxville, TN). PET data was reconstructed using the OSEM algorithm on a 4D volume ([^{18}F]AZD4694, 3x600s; [^{18}F]MK6240, 4x300s). SUVR maps were generated using the cerebellar GM as reference region for [^{18}F]AZD4694 and the inferior cerebellar GM for [^{18}F]MK6240. PET images were spatially smoothed to achieve a final resolution of 8mm FWHM. T1-weighted images were acquired at 3T for co-registration purposes and were corrected for non-uniformity and field-

distortion using an in-house pipeline.

Statistical analysis

The statistical software R (version 3.4.3) was used to perform statistical tests for demographic comparisons and data description. The R packages *lm* and *nlme* were used to perform linear models and linear mixed effect (LME) based analyses, respectively. Cross-sectional data from ADNI and TRIAD were independently analysed with linear models. LME models were used only with longitudinal ADNI data to compare the progression in plasma NfL between CU and CI subjects; this model had plasma NfL as the dependent variable and included the main effects and the interaction between the independent variables time (days between baseline NfL and follow-up time points) and group and were adjusted for sex, age at initial NfL, with random intercepts accounting for the time correlation within subjects. 95% confidence intervals were determined based on the estimated fitted value across the distribution from 1000 simulations of the model (including all variations, except theta). Statistical significance was set at $P<0.05$, two-sided.

The voxel-wise analysis also involved longitudinal and cross-sectional data. For the longitudinal data (ADNI only), two additional LME models were implemented. The first model addressed the longitudinal relationship between plasma NfL (independent variable) and voxel-based morphometry (VBM; dependent variable, adjusting for time (continuous), age at initial NfL, sex, scanner type (1·5 or 3T) and the time between plasma collection and MRI, with a random intercept). The second model addressed the longitudinal association between the interaction of plasma NfL (independent variable) with time in relation to the dependent variable, VBM (adjusting for time of assessment [0, 12, 24, 36 or 48 months], age, sex, scanner type [1·5 or 3T]) and a correction factor for time-gaps between plasma collection and MRI acquisitions. Voxel-based GM and WM morphometric analyses were performed for CU and CI groups separately. Finally, voxel-wise linear models examined the cross-sectional

associations between plasma NfL (predictor) and Aβ or tau PET (dependent variables). These models were first applied in ADNI and then subsequently reassessed in the TRIAD cohort. The linear models included corrections for either Aβ or tau (i.e. models with tau PET as the outcome were adjusted for global Aβ and vice-versa), and age, sex and time interval between plasma and PET.

All voxel-wise analyses were performed using VoxelStats (Mathotaarachchi *et al.*, 2016) and findings were corrected for multiple comparisons using random field theory. Since we hypothesized that elevated plasma NfL would be associated with elevated Aβ and tau PET and decreased brain volume using VBM, one-tailed hypothesis tests with a type I error $\alpha<0.05$ were performed.

For complete details on the statistical models and voxel-wise analyses, see the appendix, p5.

Data availability

Raw data are available for download upon request at http://adni.loni.usc.edu. Derived data supporting the findings of this study are available from the corresponding author on request.

Results

Demographic characteristics

A total of 1265 subjects were included in the present study (for study design and information about the cohorts, see the appendix, p 2). From the ADNI cohort, 1149 subjects were included; of these, 215 had only baseline data available. The initial plasma NfL concentrations were on average higher in the CI group compared to the CU group (t=6·65; P<0·0001; Fig. 2A), adjusting for age and sex. Plasma NfL was highly associated with age (t=19·50; P<0·0001), but not with sex, education or *APOE* ε4 status when adjusting for diagnosis. In the TRIAD

cohort, comprising 116 participants with cross-sectional data, CI participants had higher levels of plasma NfL (t=2·55; P=0·011; Fig. 2B), as compared to CU participants. Similar to ADNI, age had a large effect on plasma NfL (t=4·23; P<0·0001) but sex, education and *APOE* ε4 status (when adjusting for diagnosis), did not.

When using longitudinal data from ADNI, the LME analysis showed that plasma NfL differed between groups over time (t_{groups}=6·58, P<0·0001; Fig. 2C). However, no difference was found between the slopes ($t_{interaction\ (groups*time)}$=1·40; P=0·16), indicating that the rate of increase in plasma NfL levels did not differ between groups (plasma NfL time-point correlations are presented in appendix, p6). Comparison of plasma NfL concentrations in CU and CI by Aß-status showed that Aß positive subjects had higher concentrations of plasma NfL cross-sectionally (appendix, p10) and a steeper rate of progression over time, as compared to Aß negative subjects (appendix, pp 11-12).

Plasma NfL is associated with Aβ and tau in AD related brain areas

The cross-sectional voxel-wise analysis showed an association between plasma NfL and [^{18}F]florbetapir in CU participants (Fig. 3A; ADNI, $t_{(103)}$ and TRIAD, $t_{(67)}$>3·21, both P<0·05). These associations were seen primarily in the posterior cingulate/precuneus, parietal cortex, frontal and temporal cortices (peak t-values, along with their coordinates/exact p-values, and effect size information, are available in the appendix, pp7-9). No significant associations were seen between plasma NfL and amyloid PET among CI subjects.

In ADNI, [^{18}F]flortaucipir showed some association with plasma NfL in the CI group ($t_{(79)}$>3·19, P<0·05; Fig. 3B), although these results did not survive multiple comparison correction. In the TRIAD cohort, tau-load ([^{18}F]MK6240) and plasma NfL were associated only in the CI group ($t_{(35)}$>3·34, P<0·05), showing strong associations in the frontal and temporal regions.

Plasma NfL is associated with gray matter atrophy in AD related brain areas in *APOE* ε4 carriers.

The voxel-wise LME (adjusted for time and other covariates) demonstrated increases in plasma NfL levels associated with reduced GM volume in CU ($t_{(1000)}$<-3·09, P<0·05; Fig. 4A) and CI participants ($t_{(1969)}$<-3·09, P<0·05; Fig. 4B). Associations in the CU group were confined to small clusters in the frontal lobe and hippocampus. Among CI participants, more widespread associations were seen in frontal and temporal cortices, as well as in the medial temporal lobe.

Given the above described association between plasma NfL and amyloid PET in CU subjects, CU and CI groups were subdivided according to *APOE* ε4 status due to ε4 carriers being more likely having Aβ accumulation (Morris, Roe et al. 2010, Fleisher, Chen et al. 2013). When doing so, a clear distinction was seen between *APOE* ε4 carriers and non-carriers among CU subjects, with findings localized in the frontal, posterior cingulate and temporal cortices of ε4 carriers only ($t_{(260)}$<-3·12, P<0·05) and no associations found in ε4 non-carriers. Among CI subjects, no clear differences were seen between *APOE* ε4 carriers and non-carriers, with both groups showing significant associations between plasma NfL and GM volume ($t_{carriers\ (1009)}$<-3·09, $t_{non\text{-}carriers\ (951)}$<-3·09, P<0·05), mainly in the temporal cortices. *APOE* ε4 carriers, however, appeared to have more medial temporal atrophy.

When examining the association between GM volume and plasma NfL over time (NfL interaction with time), CU subjects only showed significant findings for the contrast baseline versus 48 months ($t_{(993)}$<-3·09, P<0·05; Fig. 4C), with results seen primarily in the frontal and temporal cortices. CI subjects, by contrast, showed a progressive reduction in GM volume associated with increased plasma NfL, predominantly in the temporal cortex ($t_{(1962)}$<-3·09, P<0.05; Fig. 4D).

Plasma NfL correlates with white matter atrophy

In addition to GM loss, increases in plasma NfL concentrations were accompanied by a reduction in WM volume. Using voxel-wise LME (adjusted for time and other covariates), CU participants showed significant associations between plasma NfL and WM volume in the hippocampus, parietal and prefrontal cortices ($t_{(1005)}$<-3·09, P<0·05; Fig. 5A); these findings were very focal, however. By contrast, widespread associations were seen within the CI group ($t_{(1947)}$<-3·09, P<0·05). When the LME tested the effect of NfL and time (interaction) on WM, plasma NfL was found to associate with WM volume in superior periventricular areas in the CU group ($t_{(998)}$<-3·09, P<0·05; Fig. 5B). Only at month 36, however, was it possible to detect clear findings in temporal regions. In the CI group, by contrast, these associations were seen at 12-months in temporal regions ($t_{(1940)}$<-3·09, P<0·05; Fig. 5C) and spread across the additional time points.

Discussion

The present study, to our knowledge, is the first to examine the associations between plasma NfL and whole brain imaging measures of Aβ, tau pathology and atrophy (GM and WM). Consistent with previous work (Sjogren *et al.*, 2000; Mattsson *et al.*, 2017; Ashton *et al.*, 2019; Mattsson *et al.*, 2019), we showed a linear increase in plasma NfL levels from CU controls through MCI and AD. Our main finding was that the associations between NfL, the aggregation of Aβ and tau, and brain atrophy, were disease stage specific. Specifically, while a positive correlation was observed between plasma NfL and Aβ PET in CU participants, NfL was found to correlate with tau PET in CI patients. We also observed that NfL and GM atrophy associations, found in CU and CI individuals, were dependent on *APOE* ε4 status only in CU individuals. Importantly, these associations predominantly occurred in voxels within AD-related brain areas. Despite longitudinal increases in plasma NfL, its association with GM

volume loss was only evident at 48 months in CU subjects, while in CI subjects the association between NfL and GM volume progressively increased over 48 months. In CU subjects, NfL was also associated with small foci of WM atrophy in the anterior and posterior cingulate as well as the angular bundle, contrasting with a more global pattern of WM atrophy in CI subjects. In fact, the longitudinal associations between plasma NfL and WM atrophy progressively involved the entire periventricular region in CU subjects, in contrast to CI subjects, where the more widespread findings observed at 48 months seemed to have propagated from the temporal lobe.

The observed relationship between plasma NfL and Aβ load among CU subjects was in agreement with the existing literature. Although a negligible degree of neuronal injury has been reported in preclinical AD (*i.e.*, Aβ-positive CU) (Mattsson *et al.*, 2017), our results corroborate the framework proposing that the initial neural injury in AD pathophysiology, here indexed by plasma NfL, is linked to the accumulation of Aβ, rather than tau (Mielke *et al.*, 2019). Another study demonstrated that baseline plasma NfL among CU subjects did not relate significantly to Aβ accumulation over a short follow-up interval, although increases in plasma NfL tracked increased signal from Aβ PET (Mielke *et al.*, 2019). In addition, the brain regions found here to be linking Aβ to neurodegeneration in CU are frequently reported as having high levels of Aβ in AD (Grothe *et al.*, 2017). This scenario would prove consistent with the topographical overlap we observed between areas showing significant associations between plasma NfL and amyloid PET (*e.g.*, the temporal cortex and precuneus), and areas showing declines in GM volume. Similarly, one study has shown that the association between NfL and Aβ was also accompanied by declines in hippocampal volume and global cortical thickness and speculated that the observed association with amyloid PET may reflect AD-related neurodegeneration (Mielke *et al.*, 2019). The observed association between plasma NfL levels and hippocampal WM atrophy supports previous work showing that WM integrity in this

structure is affected early on in the course of AD (Salat *et al.*, 2010), likely due to the accumulation of tau pathology (Jacobs *et al.*, 2018).

In contrast to the CU group, plasma NfL associations were confined to tau PET among CI subjects. While there are to date no other studies that have employed tau PET when looking at plasma NfL in both CU and CI groups, a recent study in CI subjects reported associations between plasma NfL and tau PET similar to those presented herein (Thijssen *et al.*, 2020). In addition, previous work has shown plasma NfL to positively correlate with CSF phosphorylated tau (P-tau) over time in subjects with CI (Mattsson *et al.*, 2019). Similar findings have also been reported using NfL from cross-sectional plasma and CSF samples (Zetterberg *et al.*, 2016; Pereira *et al.*, 2017). The fact that the association was specific to tau in the CI group may reflect CI subjects showing continued accumulation of tau pathology (McDade and Bateman, 2018), in contrast to Aβ deposition, which is thought to plateau during the symptomatic course of AD (Jack *et al.*, 2013b). Voxel-wise associations between plasma NfL and tau PET differed between cohorts, however, with findings that did not survive multiple comparison correction in ADNI, in contrast to robust positive associations within frontotemporal regions in the TRIAD cohort. This observed difference may relate to differing time intervals between plasma sampling and tau PET between cohorts. Although models accounted for this difference, this, combined with [^{18}F]flortaucipir and [^{18}F]MK6240 differing in their sensitivity to tau aggregates (Hostetler, Walji et al. 2016), may account for the observed discrepancy. In addition, as compared to ADNI, the TRIAD cohort included patients with more advanced disease stage, as evidenced by CDR ranges; this may have influenced our findings. Overall, however, the overlap of NfL-associated brain regions between cohorts and in comparison with previously reported findings (Thijssen *et al.*, 2020) suggests that the reported associations are valid.

The discrepancies in the association of plasma NfL with Aβ and tau PET in the CU and CI groups, as discussed above, are in line with the literature suggesting a pathophysiological model for AD in which Aβ biomarkers become abnormal earlier than tau biomarkers (Jack *et al.*, 2013a). Both processes, however, are upstream from neurodegeneration. This may partially explain the differential association observed between plasma NfL and PET findings across groups. Importantly, however, our findings remain correlational at the cross-sectional level and cannot support any claims of causality.

Using VBM, plasma NfL was found to associate with both GM and WM volume loss in CU and CI subjects. Using GM VBM data, though findings were limited when looking across all CU subjects, analysis by *APOE* subgroups (ε4 carriers and non-carriers) showed significant declines in GM volume in temporal, posterior cingulate and orbitofrontal regions among ε4 carriers. As described above, these findings overlapped spatially with areas that showed a significant association between plasma NfL and Aβ imaging and may be due to *APOE* ε4 carriers showing enhanced Aβ deposition (Reiman *et al.*, 2009). Reinforcing this idea, we have shown in a recent study (Benedet *et al.*, 2019) that neurodegeneration in CU subjects, indexed by reduced [^{18}F]fluorodeoxyglucose PET uptake, was only associated with NfL in Aβ positive individuals, displaying regional associations similar to those described above. Longitudinally, only at 48-months, however, was the relationship between GM VBM and plasma NfL seen to progress. This suggests a temporal delay between the build-up of Aβ pathology and neuronal injury. As hypothesized, among CI subjects, the coupling between NfL and GM loss was more pronounced, particularly within the temporal lobe, and showed a continuous increase across time points. Moreover, associated areas overlapped with those showing significant associations between plasma NfL and tau PET. These findings are consistent with neuroimaging studies showing progressive neuronal loss across the symptomatic phase of AD (Jack *et al.*, 2004) and the co-localization of tau and neurodegeneration (Benedet *et al.*, 2019). Not surprisingly, no

notable difference was seen in the GM associations between CI *APOE* ε4 carriers and non-carriers. As expected, at this disease stage the majority of the subjects showed evidence of amyloidosis and neurodegeneration, regardless of their *APOE* ε4 status.

In addition to the loss of cortical neurons, WM injury (Migliaccio *et al.*, 2012) and the loss of cortico-subcortical connectivity (Delbeuck *et al.*, 2003) are features of AD. In CU and CI subjects, the extent of WM volume loss exceeded that of GM loss. This finding is also in agreement with early CSF studies showing an association between NfL and CT measures of WM changes (Sjogren *et al.*, 2001). Since plasma NfL levels are understood to reflect damage to large-caliber myelinated axons (Ashton *et al.*, 2019), this would suggest that WM damage may precede GM loss in AD. Indeed, there is evidence to support the position that WM abnormalities precede GM changes: CSF Aβ levels correlate with WM lesions in cognitively normal elderly (Skoog *et al.*, 2018), and changes in CSF tau measures and $A\beta_{1-42}$ have been shown to predict MR based measures of WM integrity in CU individuals at risk for AD in the absence of effects on GM (Bendlin *et al.*, 2012). Moreover, soluble Aβ is toxic to oligodendrocytes (Lee *et al.*, 2004) and elevated in the WM (Collins-Praino *et al.*, 2014). Further, while the neocortical tau pathology seen in AD mainly affects GM, glial tangles are also seen in oligodendroglia (Ballatore *et al.*, 2007) and phosphorylated tau in GM has been shown to be associated with demyelination and WM abnormalities in AD (McAleese *et al.*, 2017). Aβ and tau may thus first result in WM damage, as reflected by increases in plasma NfL, which subsequently result in GM loss but with a spatiotemporally offset course.

This study has limitations. First, we did not account for vascular burden in our analyses, which may limit the interpretation of findings. In addition, the ADNI and TRIAD cohorts used for cross-sectional analyses differed in sample size, in the average time interval between plasma and PET measurements, and in the PET tracers used. While the difference in the time between plasma and PET was accounted for in statistical models, this may have affected the

comparability of findings between CI groups. Furthermore, even though plasma NfL measurements for both ADNI and TRIAD were performed in the same laboratory employing the same *in-house* assay, different batches of reagents were utilized in these studies, resulting in plasma NfL levels being higher in ADNI as compared to TRIAD; this difference was confirmed by evaluating the internal controls used, which were the same in both analyses. Despite these differences, however, it is important to stress that results were quite similar between cohorts. Moreover, a larger sample size combined with the inclusion of non-AD subjects and longitudinal PET data would have allowed us to have a detailed investigation of the ability of plasma NfL to capture the neurodegenerative effects of both Aβ and tau, as well as aspects of neuronal damage that are non-related to either proteinopathy. Lastly, though not the aim of this study, the current study design precludes us teasing apart the exact contributions of Aβ, tau and neurodegeneration to plasma NfL levels.

In conclusion, the present findings suggest that plasma NfL may prove a marker of early Aβ-related neuronal injury in AD at its presymptomatic stage, being in turn more closely related to tau-mediated neurodegeneration during the symptomatic course of the disease. Further, the association of elevated plasma NfL to widespread GM and WM loss provides further evidence supporting the use of NfL as marker of progressive neuronal damage.

Acknowledgements

Data collection and sharing for this project was funded by the Alzheimer's Disease Neuroimaging Initiative (ADNI) (National Institutes of Health Grant U01 AG024904) and DOD ADNI (Department of Defense award number W81XWH-12-2-0012). ADNI is funded by the National Institute on Aging, the National Institute of Biomedical Imaging and Bioengineering, and through generous contributions from the following: AbbVie, Alzheimer's Association; Alzheimer's Drug Discovery Foundation; Araclon Biotech; BioClinica, Inc.; Biogen; Bristol-Myers Squibb Company; CereSpir, Inc.; Cogstate; Eisai Inc.; Elan Pharmaceuticals, Inc.; Eli Lilly and Company; EuroImmun; F. Hoffmann-La Roche Ltd and its affiliated company Genentech, Inc.; Fujirebio; GE Healthcare; IXICO Ltd.; Janssen Alzheimer Immunotherapy Research & Development, LLC.; Johnson & Johnson Pharmaceutical Research & Development LLC.; Lumosity; Lundbeck; Merck & Co., Inc.; Meso Scale Diagnostics, LLC.; NeuroRx Research; Neurotrack Technologies; Novartis Pharmaceuticals Corporation; Pfizer Inc.; Piramal Imaging; Servier; Takeda Pharmaceutical Company; and Transition Therapeutics. The Canadian Institutes of Health Research is providing funds to support ADNI clinical sites in Canada. Private sector contributions are facilitated by the Foundation for the National Institutes of Health (www.fnih.org). The grantee organization is the Northern California Institute for Research and Education, and the study is coordinated by the Alzheimer's Therapeutic Research Institute at the University of Southern California. ADNI data are disseminated by the Laboratory for Neuro Imaging at the University of Southern California.

Funding

This work was also supported by the Canadian Institutes of Health Research (CIHR) (MOP-11-51-31), the Alzheimer's Association (NIRG-08-92090), Canadian Consortium of Neurodegeneration in Aging (CIHR-CCNA) and the Weston Brain Institute. Andréa L. Benedet is supported by the CAPES Foundation - Brazil [0327/13-1]. NJA is funded by the Wallenberg Centre for Molecular and Translational Medicine. Kaj Blennow is supported by the Torsten Söderberg Foundation, Stockholm, Sweden, is supported by the Swedish Research Council (#2017-00915), the Swedish Alzheimer Foundation (#AF-742881), Hjärnfonden, Sweden (#FO2017-0243), and a grant (#ALFGBG-715986) from the Swedish state under the agreement between the Swedish government and the County Councils, the ALF-agreement. Henrik Zetterberg is a Wallenberg Scholar supported by grants from the Swedish Research Council (#2018-02532), the European Research Council (#681712), Swedish State Support for Clinical Research (#ALFGBG-720931) and the UK Dementia Research Institute at UCL. Pedro Rosa-Neto is supported by the Fonds de la recherche en santé du Québec (chercheur boursier), and. Serge Gauthier and Pedro Rosa-Neto are members of the CIHR Canadian Consortium of Neurodegeneration in Aging.

Competing interests

Kaj Blennow has served as a consultant or on advisory boards for Alector, Alzheon, CogRx, Biogen, Lilly, Novartis and Roche Diagnostics, and is a co-founder of Brain Biomarker Solutions in Gothenburg AB (BBS), which is a part of the GU Ventures Incubator Program, all unrelated to the submitted work. Henrik Zetterberg has served at scientific advisory boards for Denali, Roche Diagnostics, Wave, Samumed, Siemens Healthineers, Pinteon Therapeutics and CogRx, has given lectures in symposia sponsored by Fujirebio, Alzecure and Biogen, and

is a co-founder of Brain Biomarker Solutions in Gothenburg AB (BBS), which is a part of the GU Ventures Incubator Program, all unrelated to the submitted work.

References

Ashton NJ, Leuzy A, Lim YM, Troakes C, Hortobagyi T, Hoglund K, *et al.* Increased plasma neurofilament light chain concentration correlates with severity of post-mortem neurofibrillary tangle pathology and neurodegeneration. Acta Neuropathol Commun 2019; 7(1): 5.

Ballatore C, Lee VM, Trojanowski JQ. Tau-mediated neurodegeneration in Alzheimer's disease and related disorders. Nat Rev Neurosci 2007; 8(9): 663-72.

Bendlin BB, Carlsson CM, Johnson SC, Zetterberg H, Blennow K, Willette AA, *et al.* CSF T-Tau/Abeta42 predicts white matter microstructure in healthy adults at risk for Alzheimer's disease. PLoS One 2012; 7(6): e37720.

Benedet AL, Ashton NJ, Pascoal TA, Leuzy A, Mathotaarachchi S, Kang MS, *et al.* Plasma neurofilament light associates with Alzheimer's disease metabolic decline in amyloid-positive individuals. Alzheimers Dement (Amst) 2019; 11: 679-89.

Bridel C, van Wieringen WN, Zetterberg H, Tijms BM, Teunissen CE, and the NFLG, *et al.* Diagnostic Value of Cerebrospinal Fluid Neurofilament Light Protein in Neurology: A Systematic Review and Meta-analysis. JAMA Neurol 2019.

Chatterjee P, Goozee K, Sohrabi HR, Shen K, Shah T, Asih PR, *et al.* Association of Plasma Neurofilament Light Chain with Neocortical Amyloid-beta Load and Cognitive Performance in Cognitively Normal Elderly Participants. J Alzheimers Dis 2018; 63(2): 479-87.

Collins-Praino LE, Francis YI, Griffith EY, Wiegman AF, Urbach J, Lawton A, *et al.* Soluble amyloid beta levels are elevated in the white matter of Alzheimer's patients, independent of cortical plaque severity. Acta Neuropathol Commun 2014; 2: 83.

Delbeuck X, Van der Linden M, Collette F. Alzheimer's disease as a disconnection syndrome? Neuropsychol Rev 2003; 13(2): 79-92.

Gisslen M, Price RW, Andreasson U, Norgren N, Nilsson S, Hagberg L, *et al.* Plasma Concentration of the Neurofilament Light Protein (NFL) is a Biomarker of CNS Injury in HIV Infection: A Cross-Sectional Study. EBioMedicine 2016; 3: 135-40.

Grothe MJ, Barthel H, Sepulcre J, Dyrba M, Sabri O, Teipel SJ, *et al.* In vivo staging of regional amyloid deposition. Neurology 2017; 89(20): 2031-8.

Hampel H, O'Bryant SE, Molinuevo JL, Zetterberg H, Masters CL, Lista S, *et al.* Blood-based biomarkers for Alzheimer disease: mapping the road to the clinic. Nat Rev Neurol 2018; 14(11): 639-52.

Jack CR, Jr., Knopman DS, Jagust WJ, Petersen RC, Weiner MW, Aisen PS, *et al.* Tracking pathophysiological processes in Alzheimer's disease: an updated hypothetical model of dynamic biomarkers. Lancet Neurol 2013a; 12(2): 207-16.

Jack CR, Jr., Shiung MM, Gunter JL, O'Brien PC, Weigand SD, Knopman DS, *et al.* Comparison of different MRI brain atrophy rate measures with clinical disease progression in AD. Neurology 2004; 62(4): 591-600.

Jack CR, Jr., Wiste HJ, Lesnick TG, Weigand SD, Knopman DS, Vemuri P, *et al.* Brain beta-amyloid load approaches a plateau. Neurology 2013b; 80(10): 890-6.

Jacobs HIL, Hedden T, Schultz AP, Sepulcre J, Perea RD, Amariglio RE, *et al.* Structural tract alterations predict downstream tau accumulation in amyloid-positive older individuals. Nat Neurosci 2018; 21(3): 424-31.

Lee JT, Xu J, Lee JM, Ku G, Han X, Yang DI, *et al.* Amyloid-beta peptide induces oligodendrocyte death by activating the neutral sphingomyelinase-ceramide pathway. J Cell Biol 2004; 164(1): 123-31.

Mathotaarachchi S, Wang S, Shin M, Pascoal TA, Benedet AL, Kang MS, *et al.* VoxelStats: A MATLAB Package for Multi-Modal Voxel-Wise Brain Image Analysis. Front Neuroinform 2016; 10: 20.

Mattsson N, Andreasson U, Zetterberg H, Blennow K, Alzheimer's Disease Neuroimaging I. Association of Plasma Neurofilament Light With Neurodegeneration in Patients With Alzheimer Disease. JAMA Neurol 2017; 74(5): 557-66.

Mattsson N, Cullen NC, Andreasson U, Zetterberg H, Blennow K. Association Between Longitudinal Plasma Neurofilament Light and Neurodegeneration in Patients With Alzheimer Disease. JAMA Neurol 2019; 76(7): 791-9.

McAleese KE, Walker L, Graham S, Moya ELJ, Johnson M, Erskine D, *et al.* Parietal white matter lesions in Alzheimer's disease are associated with cortical neurodegenerative pathology, but not with small vessel disease. Acta Neuropathol 2017; 134(3): 459-73.

McDade E, Bateman RJ. Tau Positron Emission Tomography in Autosomal Dominant Alzheimer Disease: Small Windows, Big Picture. JAMA Neurol 2018; 75(5): 536-8.

McKhann G, Drachman D, Folstein M, Katzman R, Price D, Stadlan EM. Clinical diagnosis of Alzheimer's disease: report of the NINCDS-ADRDA Work Group under the auspices of Department of Health and Human Services Task Force on Alzheimer's Disease. Neurology 1984; 34(7): 939-44.

Mielke MM, Syrjanen JA, Blennow K, Zetterberg H, Vemuri P, Skoog I, *et al.* Plasma and CSF neurofilament light: Relation to longitudinal neuroimaging and cognitive measures. Neurology 2019; 93(3): e252-e60.

Migliaccio R, Agosta F, Possin KL, Rabinovici GD, Miller BL, Gorno-Tempini ML. White matter atrophy in Alzheimer's disease variants. Alzheimers Dement 2012; 8(5 Suppl): S78-87 e1-2.

Pereira JB, Westman E, Hansson O, Alzheimer's Disease Neuroimaging I. Association between cerebrospinal fluid and plasma neurodegeneration biomarkers with brain atrophy in Alzheimer's disease. Neurobiol Aging 2017; 58: 14-29.

Preische O, Schultz SA, Apel A, Kuhle J, Kaeser SA, Barro C, *et al.* Serum neurofilament dynamics predicts neurodegeneration and clinical progression in presymptomatic Alzheimer's disease. Nat Med 2019; 25(2): 277-83.

Quiroz YT, Zetterberg H, Reiman EM, Chen Y, Su Y, Fox-Fuller JT, *et al.* Plasma neurofilament light chain in the presenilin 1 E280A autosomal dominant Alzheimer's disease kindred: a cross-sectional and longitudinal cohort study. Lancet Neurol 2020; 19(6): 513-21.

Reiman EM, Chen K, Liu X, Bandy D, Yu M, Lee W, *et al.* Fibrillar amyloid-beta burden in cognitively normal people at 3 levels of genetic risk for Alzheimer's disease. Proc Natl Acad Sci U S A 2009; 106(16): 6820-5.

Salat DH, Tuch DS, van der Kouwe AJ, Greve DN, Pappu V, Lee SY, *et al.* White matter pathology isolates the hippocampal formation in Alzheimer's disease. Neurobiol Aging 2010; 31(2): 244-56.

Sjogren M, Blomberg M, Jonsson M, Wahlund LO, Edman A, Lind K, *et al.* Neurofilament protein in cerebrospinal fluid: a marker of white matter changes. J Neurosci Res 2001; 66(3): 510-6.

Sjogren M, Rosengren L, Minthon L, Davidsson P, Blennow K, Wallin A. Cytoskeleton proteins in CSF distinguish frontotemporal dementia from AD. Neurology 2000; 54(10): 1960-4.

Skoog I, Kern S, Zetterberg H, Ostling S, Borjesson-Hanson A, Guo X, *et al.* Low Cerebrospinal Fluid Abeta42 and Abeta40 are Related to White Matter Lesions in Cognitively Normal Elderly. J Alzheimers Dis 2018; 62(4): 1877-86.

Thijssen EH, La Joie R, Wolf A, Strom A, Wang P, Iaccarino L, *et al.* Diagnostic value of plasma phosphorylated tau181 in Alzheimer's disease and frontotemporal lobar degeneration. Nat Med 2020; 26(3): 387-97.

Trojanowski JQ, Walkenstein N, Lee VM. Expression of neurofilament subunits in neurons of the central and peripheral nervous system: an immunohistochemical study with monoclonal antibodies. J Neurosci 1986; 6(3): 650-60.

Weston PSJ, Poole T, Ryan NS, Nair A, Liang Y, Macpherson K*, et al.* Serum neurofilament light in familial Alzheimer disease: A marker of early neurodegeneration. Neurology 2017; 89(21): 2167-75.

Zetterberg H. Neurofilament Light: A Dynamic Cross-Disease Fluid Biomarker for Neurodegeneration. Neuron 2016; 91(1): 1-3.

Zetterberg H, Skillback T, Mattsson N, Trojanowski JQ, Portelius E, Shaw LM*, et al.* Association of Cerebrospinal Fluid Neurofilament Light Concentration With Alzheimer Disease Progression. JAMA Neurol 2016; 73(1): 60-7.

FIGURE LEGENDS

Figure 1. Flow diagram summarizing the study design

Longitudinal analyses were performed using data from ADNI participants only. Cross sectional analyses were performed in a subset of ADNI participants with Aβ and tau PET and validated in the TRIAD cohort. NfL=Neurofilament light; LOQ=limit of quantification; Aβ=amyloid-β; PET=positron emission tomography; VBM=voxel-based morphometry; GM=gray matter; WM=white matter. Cross-sectional analysis was performed on a subset of participants who had Aβ and tau PET matching closely with plasma NfL. TRIAD data was used to validate cross-sectional findings from ADNI.

Figure 2. Plasma NfL

Findings from linear models (adjusted by age and sex) showed that differences in plasma NfL levels were seen between cognitively unimpaired (CU) and cognitively impaired (CI) subjects in both ADNI (A) and TRIAD (B) cohorts cross-sectionally. CI participants also showed higher plasma NfL concentrations as compared to CU participants (C) longitudinally, as shown by linear mixed effect modelling.

Figure 3. Plasma NfL and PET biomarkers

T-statistical parametric maps (T-maps) superimposed on average structural MRI show brain regions where higher NfL levels were associated with higher [^{18}F]florbetapir (ADNI) and [^{18}F]AZD4694 (TRIAD) standard uptake value ratios (SUVR) in the CU group (A). In CI group (B), T-maps also show brain regions where higher NfL levels are associated with higher [^{18}F]flortaucipir (ADNI) and [^{18}F]MK6240 (TRIAD) in CI subjects. T-values that were significant after random field theory (RFT) correction for multiple comparisons are indicated in the text.

Figure 4. Plasma NfL and GM volume

T-statistical parametric maps (T-maps) superimposed on average structural MRI show brain regions where higher NfL levels were associated with reduced GM volume in CU (A) and CI (B) participants, subdivided by *APOE* ε4 status [carriers (+) or non-carriers (-)]. T-maps also show that, as compared to baseline, only at 48 months was there a reduction of GM volume associated with plasma NfL in CU subjects (C), while in the CI group differences were observed at each time point (D). T-values that were significant after random field theory (RFT) correction for multiple comparisons are indicated in the text.

Figure 5. Plasma NfL and WM volume

T-statistical parametric maps (T-maps) superimposed on average structural MRI show brain regions where higher NfL levels were associated with reduced WM volume in CU and CI participants (A). T-maps also showed that, as compared to baseline, there was a reduction of WM volume associated with plasma NfL in CU (B) and CI groups (C) at each time point (D). T-values that were significant after random field theory (RFT) correction for multiple comparisons are indicated in the text.

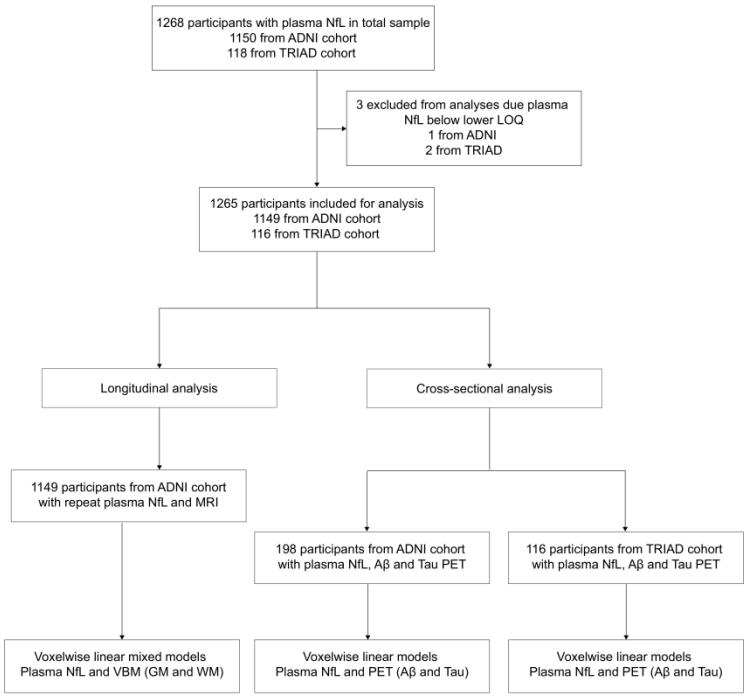

Figure 1. Flow diagram summarizing the study design
Longitudinal analyses were performed using data from ADNI participants only. Cross sectional analyses were performed in a subset of ADNI participants with Aβ and tau PET and validated in the TRIAD cohort. NfL=Neurofilament light; LOQ=limit of quantification; Aβ=amyloid-β; PET=positron emission tomography; VBM=voxel-based morphometry; GM=gray matter; WM=white matter. Cross-sectional analysis was performed on a subset of participants who had Aβ and tau PET matching closely with plasma NfL. TRIAD data was used to validate cross-sectional findings from ADNI.

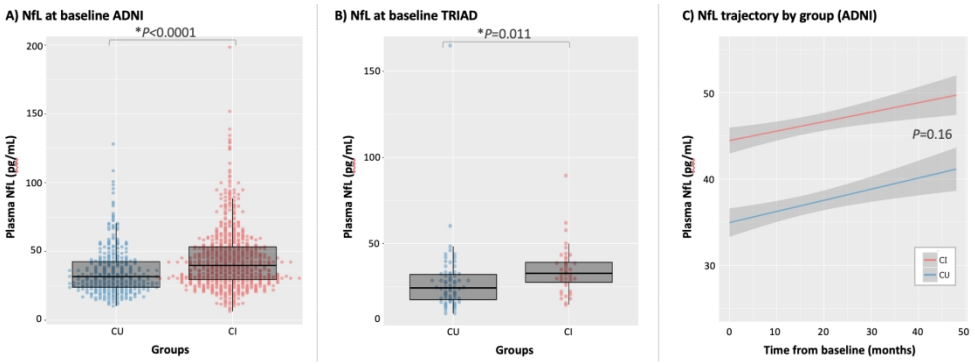

Figure 2. Plasma NfL
Findings from linear models (adjusted by age and sex) showed that differences in plasma NfL levels were seen between cognitively unimpaired (CU) and cognitively impaired (CI) subjects in both ADNI (A) and TRIAD (B) cohorts cross-sectionally. CI participants also showed higher plasma NfL concentrations as compared to CU participants (C) longitudinally, as shown by linear mixed effect modelling.

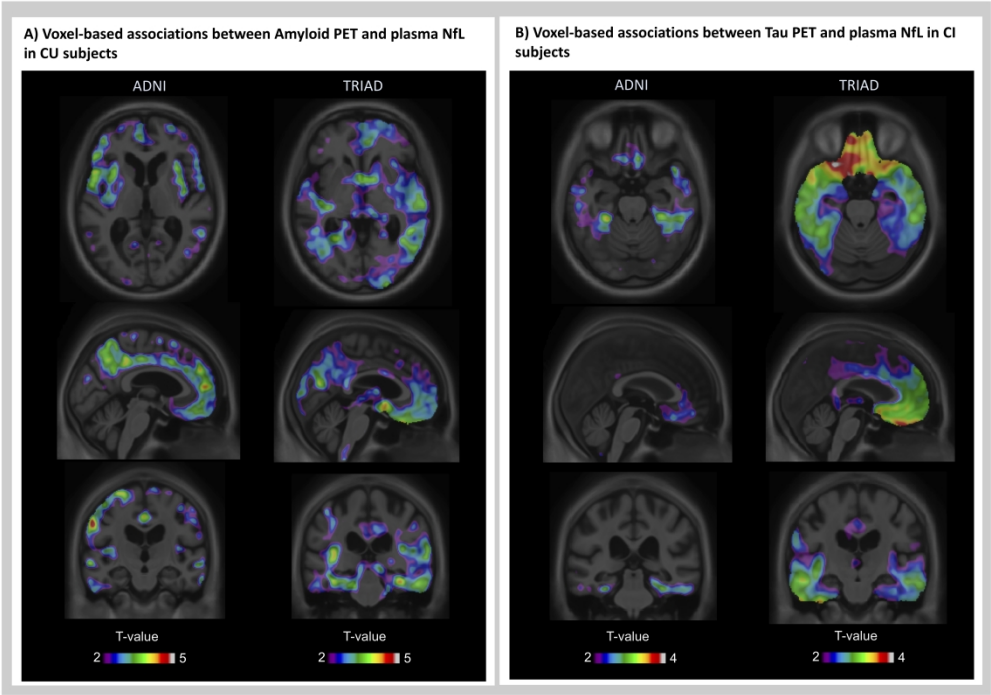

Figure 3. Plasma NfL and PET biomarkers
T-statistical parametric maps (T-maps) superimposed on average structural MRI show brain regions where higher NfL levels were associated with higher [18F]florbetapir (ADNI) and [18F]AZD4694 (TRIAD) standard uptake value ratios (SUVR) in the CU group (A). In CI group (B), T-maps also show brain regions where higher NfL levels are associated with higher [18F]flortaucipir (ADNI) and [18F]MK6240 (TRIAD) in CI subjects. T-values that were significant after random field theory (RFT) correction for multiple comparisons are indicated in the text.

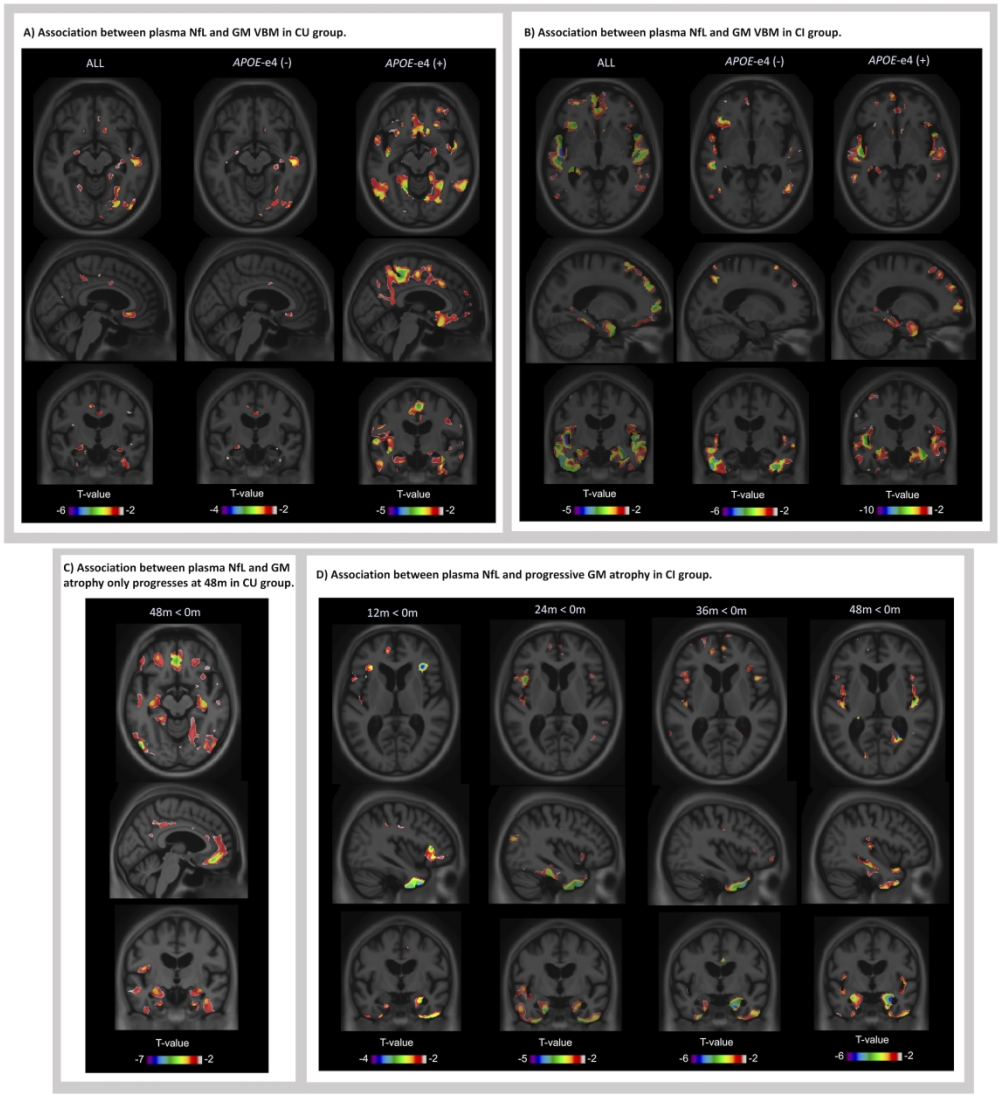

Figure 4. Plasma NfL and GM volumeT-statistical parametric maps (T-maps) superimposed on average structural MRI show brain regions where higher NfL levels were associated with reduced GM volume in CU (A) and CI (B) participants, subdivided by APOE ε4 status [carriers (+) or non-carriers (-)]. T-maps also show that, as compared to baseline, only at 48 months was there a reduction of GM volume associated with plasma NfL in CU subjects (C), while in the CI group differences were observed at each time point (D). T-values that were significant after random field theory (RFT) correction for multiple comparisons are indicated in the text.

221x246mm (500 x 500 DPI)

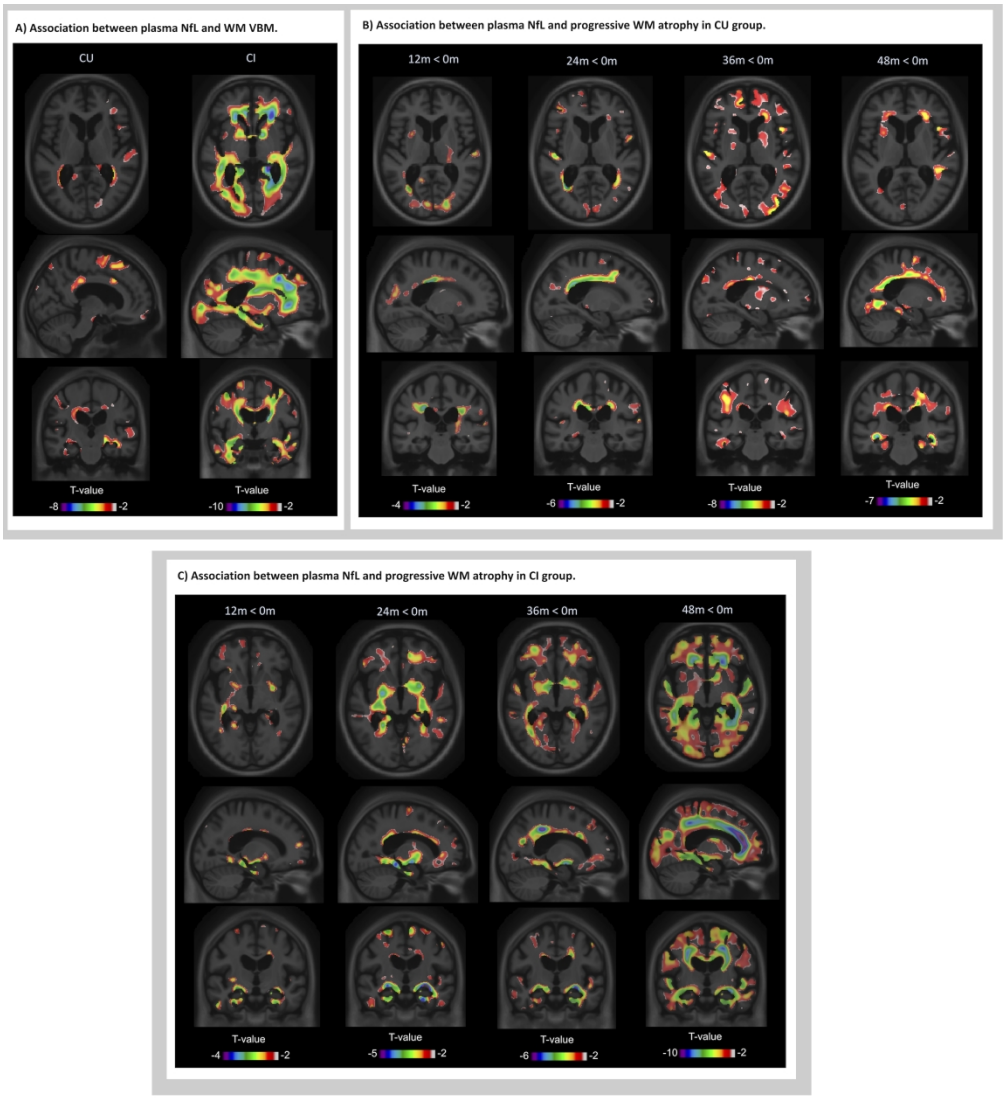

Figure 5. Plasma NfL and WM volume
T-statistical parametric maps (T-maps) superimposed on average structural MRI show brain regions where higher NfL levels were associated with reduced WM volume in CU and CI participants (A). T-maps also showed that, as compared to baseline, there was a reduction of WM volume associated with plasma NfL in CU (B) and CI groups (C) at each time point (D). T-values that were significant after random field theory (RFT) correction for multiple comparisons are indicated in the text.

Table 1. Demographics and key characteristics of the ADNI and TRIAD cohorts.

	ADNI				TRIAD		
	CU	**CI**	**p value***		**CU**	**CI**	**p value***
No. subjects	382 (33·2%)	767 (66·7%)	NA		74 (63·7%)	42 (36·2%)	NA
Age[1]	73·5 (6·9)	74·4 (7·8)	0·05		72·4 (6·2)	70·4 (8·5)	0·15
Males	173 (45·3%)	456 (59·5%)	<0·001		24 (32·4%)	21 (50·0%)	0·09
Education[1]	16·6 (2·5)	15·9 (2·7)	<0·001		15·3 (4·2)	13·7 (3·8)	0·04
APOE-ε4	106 (27·7%)	395 (51·6%)	<0·001		25 (33·8%)	17 (40·5%)	0·10
MMSE	29·0 (1·1)	26·4 (3·4)	<0·001		28·9 (1·3)	23·4 (5·3)	<0·001
Plasma NfL[2]	35·2 (16·7)	44·0 (22·2)	<0·001		27·3 (19·2)	34·5 (13·7)	0·01

Data are mean (SD) or n (%); NA Not applicable; MMSE Mini-Mental State Examination.
[1]Measured in years; [2]Measured in ng/L.
*P values were calculated comparing CU and CI subjects, within each cohort, using t-test for continuous variables and Chi-square test for categorical variables.

Supplementary Appendix

Stage-specific associations between plasma neurofilament light and biomarkers of Alzheimer's disease pathophysiology

Contents

1. Detailed description of the study populations

This study used data from the Alzheimer's disease Neuroimage Initiative (ADNI) and the Translational Biomarkers in Aging and Dementia (TRIAD) cohorts. The ADNI is a longitudinal multicentric study launched in 2003 as a public-private partnership, led by Principal Investigator Michael W. Weiner, MD. The primary goal of ADNI has been to test whether serial magnetic resonance imaging (MRI), positron emission tomography (PET), other biological markers, and clinical and neuropsychological assessments can be combined to measure the progression of mild cognitive impairment (MCI) and early Alzheimer's disease (AD). Participants are recruited since 2004 in several centers across North America. For up-to-date information about ADNI's inclusion criteria, participant's milestones and study protocols (see www.adni-info.org).

The TRIAD is an observational longitudinal and biomarker-based cohort designed to study the pathophysiological processes underlying dementia disorders. Participants, mostly ranging in the AD spectrum, are recruited at the McGill University Research Centre for Studies in Aging (Montreal-Canada catchment area) since 2017, where they are followed yearly with clinical and neuropsychological assessments, as well as with collection of fluid and acquisition of imaging biomarkers. Information about TRIAD's inclusion criteria and data collection can be found at http://triad.tnl-mcgill.com.

2. Detailed description of plasma measurements.

For both cohorts, plasma NfL concentrations were measured using an in-house immunoassay on the Single molecule array (Simoa) platform with a 4-fold dilution, as previously described[1].

In ADNI, one sample did not range between the limits of quantification (LOQ; lower LOQ=6.7 ng/L; higher LOQ=1620.0 ng/L) and was excluded. In TRIAD, two samples were below the lower LOQ (6.7 ng/L) and were removed from the analysis. In ADNI, the intra-assay coefficients of variation (CV) were 6.2% and 4.9% for the low (LCS) and high-concentration (HCS) quality control samples respectively. In TRIAD, the intra-assay CV was 5.3% for LCS and 3.4% for the HCS. The inter-assay CV in ADNI were 9.0% and 7.2% for the LCS and HCS, respectively, while in TRIAD they were 5.4% and 6.2%.

References

1. Mattsson N, Andreasson U, Zetterberg H, Blennow K, Alzheimer's Disease Neuroimaging I. Association of Plasma Neurofilament Light With Neurodegeneration in Patients With Alzheimer Disease. *JAMA neurology* 2017; **74**(5): 557-66.

3. Detailed description of imaging analysis

Pre-processed 1.5T and 3T T1-weighted MRI scans were downloaded from the ADNI database (adni.loni.usc.edu; for pre-processing details, see[1]). Anatomical images were segmented into probabilistic gray matter (GM) and white matter (WM) maps using the SPM12 segmentation tool. Each GM and WM probability map was then non-linearly registered (with modulation) to the ADNI template using DARTEL[2], and smoothed with a Gaussian kernel of full width half maximum (FWHM) of 8 mm. All images were visually inspected to insure proper alignment to the ADNI template. [^{18}F]Florbetapir and [^{18}F]flortaucipir PET images were acquired and processed as described by Landau et al. [3,4] and Schöll et al.,[5] respectively. In brief, data was acquired 50-70 min and 80-100 min, post-injection, respectively, spatially aligned, averaged and interpolated to a standard voxel size (1.5 x 1.5 x 1.5mm), and smoothed to a common resolution (8mm full width at half maximum).[6] Standard uptake value ratio (SUVR) images were then created using the cerebellar cortex ([^{18}F]florbetapir) and inferior cerebellum ([^{18}F]flortaucipir)[7] as reference regions.

In TRIAD, T1-weighted images were acquired at 3T for all participants for coregistration purposes. PET scans were acquired with a Siemens High Resolution Research Tomograph. Aβ PET was indexed using [^{18}F]AZD4694 and images were acquired 40–70 minutes post-injection. Scans were reconstructed using the ordered subset expectation maximization (OSEM) algorithm on a 4-dimensional volume with 3 frames (3 x 600s). [^{18}F]MK6240, acquired 90–110 minutes post-injection, was used to index tau load. Data was also reconstructed using the OSEM algorithm on a 4D volume with 4 frames (4 x 300s). After each acquisition, a transmission scan was performed for attenuation correction. Additional pre-processing corrections were performed as described elsewhere.[8] PET images were linearly and non-linearly registered to the ADNI template space and then spatially smoothed to achieve a final resolution of 8mm FWHM. SUVR was calculated using the cerebellar grey and the inferior cerebellar grey matter as reference regions for [^{18}F]AZD4694 and [^{18}F]MK6240, respectively.

References

1. Jack CR, Jr., Bernstein MA, Fox NC, et al. The Alzheimer's Disease Neuroimaging Initiative (ADNI): MRI methods. *J Magn Reson Imaging* 2008; **27**(4): 685-91.
2. Ashburner J. A fast diffeomorphic image registration algorithm. *Neuroimage* 2007; **38**(1): 95-113.
3. Landau SM, Mintun MA, Joshi AD, et al. Amyloid deposition, hypometabolism, and longitudinal cognitive decline. Ann Neurol 2012; 72(4): 578-86.
4. Landau SM, Breault C, Joshi AD, et al. Amyloid-beta imaging with Pittsburgh compound B and florbetapir: comparing radiotracers and quantification methods. J Nucl Med 2013; 54(1): 70-7.
5 Scholl M, Lockhart SN, Schonhaut DR, et al. PET Imaging of Tau Deposition in the Aging Human Brain. Neuron 2016; 89(5): 971-82.
6. Joshi A, Koeppe RA, Fessler JA. Reducing between scanner differences in multi-center PET studies. Neuroimage 2009; 46(1): 154-9.
7. Baker SL, Maass A, Jagust WJ. Considerations and code for partial volume correcting [(18)F]-AV-1451 tau PET data. Data Brief 2017; 15: 648-57.
8. Therriault J, Benedet AL, Pascoal TA, et al. Association of Apolipoprotein E epsilon4 With Medial Temporal Tau Independent of Amyloid-beta. JAMA Neurol 2019.

4. Detailed description of the statistical models

Cross-sectional plasma NfL levels were compared between CI and CU groups, in both cohorts, using the following linear model (LM):

$$plasma\ NfL = \beta_0 + \beta_1(groups) + covariates + \varepsilon$$

Covariates were age and sex. Additionally, a second model was applied to check the effect of age on plasma NfL, and sex, diagnosis, *APOE*-ε4 status and years of education were included as covariates.

In ADNI, a linear mixed effect (LME) model, applied on longitudinal data, checked if plasma NfL progressed differently between CI and CU groups adjusting for sex and age:

$$plasma\ NfL = \beta_0 + \beta_1(groups) + \beta_2(time\ points) + \beta_3(groups * time\ points) + covariates + (1\,|\,subject) + \varepsilon$$

For the voxel-wise analyses, LM and LME models were applied using VoxelStats,[1] a Matlab package. To investigate PET and NfL associations in each group (CU and CI), linear models were performed using cross-sectional data as follows:

$$PET_{(amyloid\ or\ tau)} = \beta_0 + \beta_1(plasma\ NfL) + \beta_2(PET_{(amyloid\ or\ tau)} + covariates + \varepsilon$$

The covariates included in this model were sex, age and time difference between plasma NfL collection and PET acquisition.

Longitudinal plasma NfL and voxel-based morphometry (VBM) maps were analyzed using LME. First LME was used to investigate the simple association between GM/WM VBM and plasma NfL accounting for individual repeated measures:

$$VBM_{(GM\ or\ WM)} = \beta_0 + \beta_1(plasma\ NfL) + covariates + (1\,|\,subject) + \varepsilon$$

This model was applied separately in CU and CI groups and included covariates were sex, years of education, age, time points (0, 12, 24, 36 and 48 months), MRI scanner type (1.5 or 3T) and time difference between plasma NfL collection and MRI acquisition, with random intercept.

A second LME tested the association between VBM and the interaction between plasma NfL and time, as described below.

$$VBM_{(GM\ or\ WM)} = \beta_0 + \beta_1(plasma\ NfL) + \beta_2(time\ points) + \beta_3(plasma\ NfL * time\ points) + covariates + (1\,|\,subject) + \varepsilon$$

Similarly to the first voxel-wise LME, this model was applied in CU and CI groups and had the same covariates. Conversely, the time points were treated here as categorical variables, in order to compare the differences against the baseline (0 months) time point.

Voxel-wise findings were corrected for multiple comparisons using Random Field Theory,[2] which accounts for imaging resolution and for the spatial correlation between voxels.

References

1. Mathotaarachchi S, Wang S, Shin M, et al. VoxelStats: a MATLAB package for multi-modal voxel-wise brain image analysis. *Frontiers in neuroinformatics* 2016; **10**.
2. Worsley KJ, Marrett S, Neelin P, Vandal AC, Friston KJ, Evans AC. A unified statistical approach for determining significant signals in images of cerebral activation. *Hum Brain Mapp* 1996; **4**(1): 58-73.

5. Presentation of time point correlations

For the longitudinal analysis we had available initial plasma NfL data from 1149 subjects, 12-months data from 798 subjects (attrition rate [AR]= 351/1149 = 30.5%), 24-months data from 618 subjects (AR= 180/798 = 22.5%), 36-months data from 209 subjects (AR= 409/618 = 66.1%) and finally, 48-months data from 195 subjects (AR= 14/209 = 6.6%).

The correlations between baseline and follow-up concentrations of plasma NfL are shown below. The correlation plots indicate that, despite the drop on sample size, the relationship of plasma NfL levels between baseline and each time point is maintained over time, which is good evidence that the data is stable.

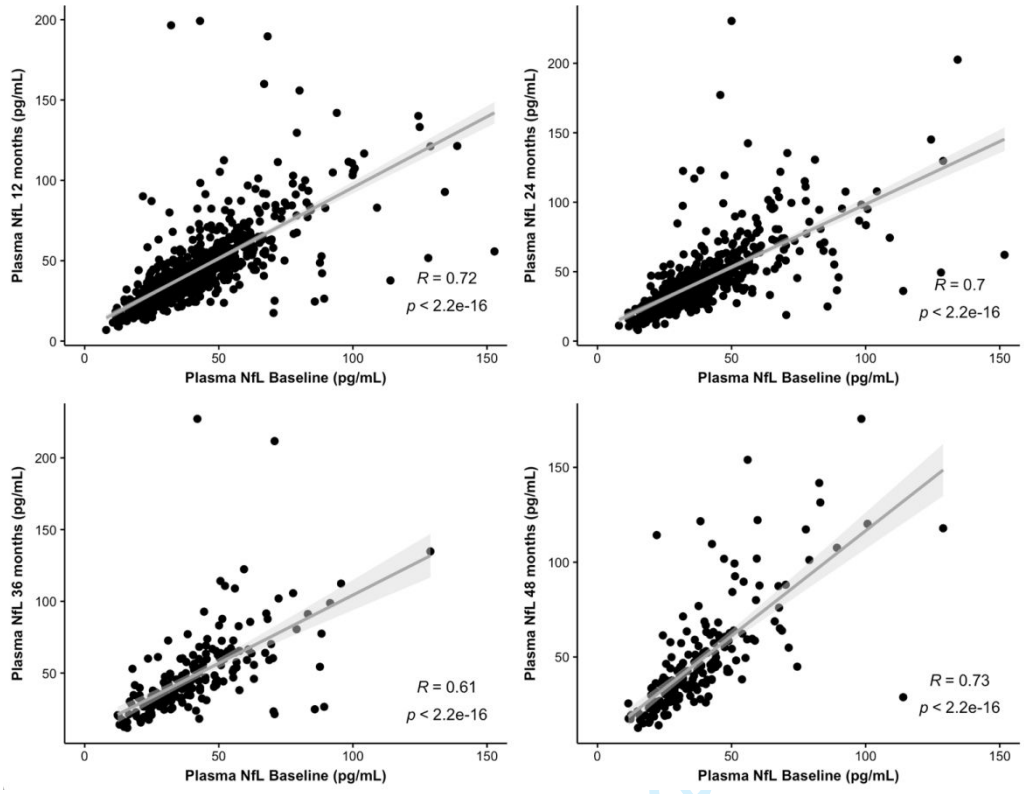

Figure S1. Correlation between plasma NfL concentrations at baseline and at each of the time points evaluated in this study.

6. Presentation of peak T-values

The table below displays, for each of the reported voxel-wise analysis, the maximum t-value, its coordinates, and the exact p-value.

Supplementary Table 1. Peak t-values, voxel world coordinates and exact p-values

Image	Peak t-value	Coordinates x	y	z	Peak p-value	Minimum p-value
Figure 2A - ADNI	5.09	-57	-20	36	8.0985E-07	0.000885227
Figure 2A - TRIAD	5.19	14	31	-25	1.06326E-06	0.001019419
Figure 2B - ADNI	4.26	45	5	-24	2.7981E-05	-
Figure 2B - TRIAD	6.11	46	35	17	2.76619E-07	0.001000123
Figure 3A - ALL	-6.23	34.94	26.52	52.85	3.43073E-10	0.001028447
Figure 3A - *APOE*- ε4(-)	-5.86	35.5	26.11	54.06	6.982E-09	0.001109468
Figure 3A - *APOE*- ε4(+)	-4.61	5.06	-39.82	56.74	2.37546E-06	0.00103868
Figure 3B - ALL	-5.01	-26.24	-3.9	-46.06	2.96459E-07	0.00101478
Figure 3B - *APOE*- ε4(-)	-4.05	-50.89	-20.97	-25.16	2.75715E-05	0.001028199
Figure 3B - *APOE*- ε4(+)	-4.98	-50	10	39	3.77439E-07	0.001029884
Figure 3C	-7.8	10.89	-32.74	41.05	7.80619E-15	0.001028644
Figure 3D - 12m<0m	-3.89	36.2	28.07	6.9	5.27358E-05	0.001022669
Figure 3D - 24m<0m	-4.7	-29.81	0.96	-48.71	1.4435E-06	0.001022669
Figure 3D - 36m<0m	-4.75	-28.75	-1	-49.12	1.1335E-06	0.001022669
Figure 3D - 48m<0m	-5.87	25.31	-53.69	4.53	2.78199E-09	0.001022669
Figure 4A - CU	-14.98	29.32	19.09	31.95	3.05268E-46	0.001028308
Figure 4A - CI	-9.27	26.79	39.1	13	5.51524E-20	0.001028308
Figure 4B - 12m<0m	-3.87	28	-11	34	5.62099E-05	0.001014939
Figure 4B - 24m<0m	-5.87	-31	-55	-19	2.55537E-09	0.001014939

Figure 4B - 36m<0m	-13.11	31	16	32	5.419E-38	0.001014939
Figure 4B - 48m<0m	-7	41.03	17.78	20.92	1.75461E-12	0.001014939
Figure 4C - 12m<0m	-4.16	-37.92	37.95	35.18	1.66069E-05	0.001014991
Figure 4C - 24m<0m	-5.39	29.14	-13.14	-12.08	3.95232E-08	0.001014991
Figure 4C - 36m<0m	-6.39	-15.81	-41.33	38.02	1.0358E-10	0.001014991
Figure 4C - 48m<0m	-10.72	-26.24	31.09	13.87	2.16967E-26	0.001014991

Peak p-values correspond to those for the peak t-value; minimum p-values correspond to the minimum p-value identified in the cluster from which the peak t-value was drawn. The dashed cell (-) indicates a lack of statistical significance for that given cluster.

7. Effect size information

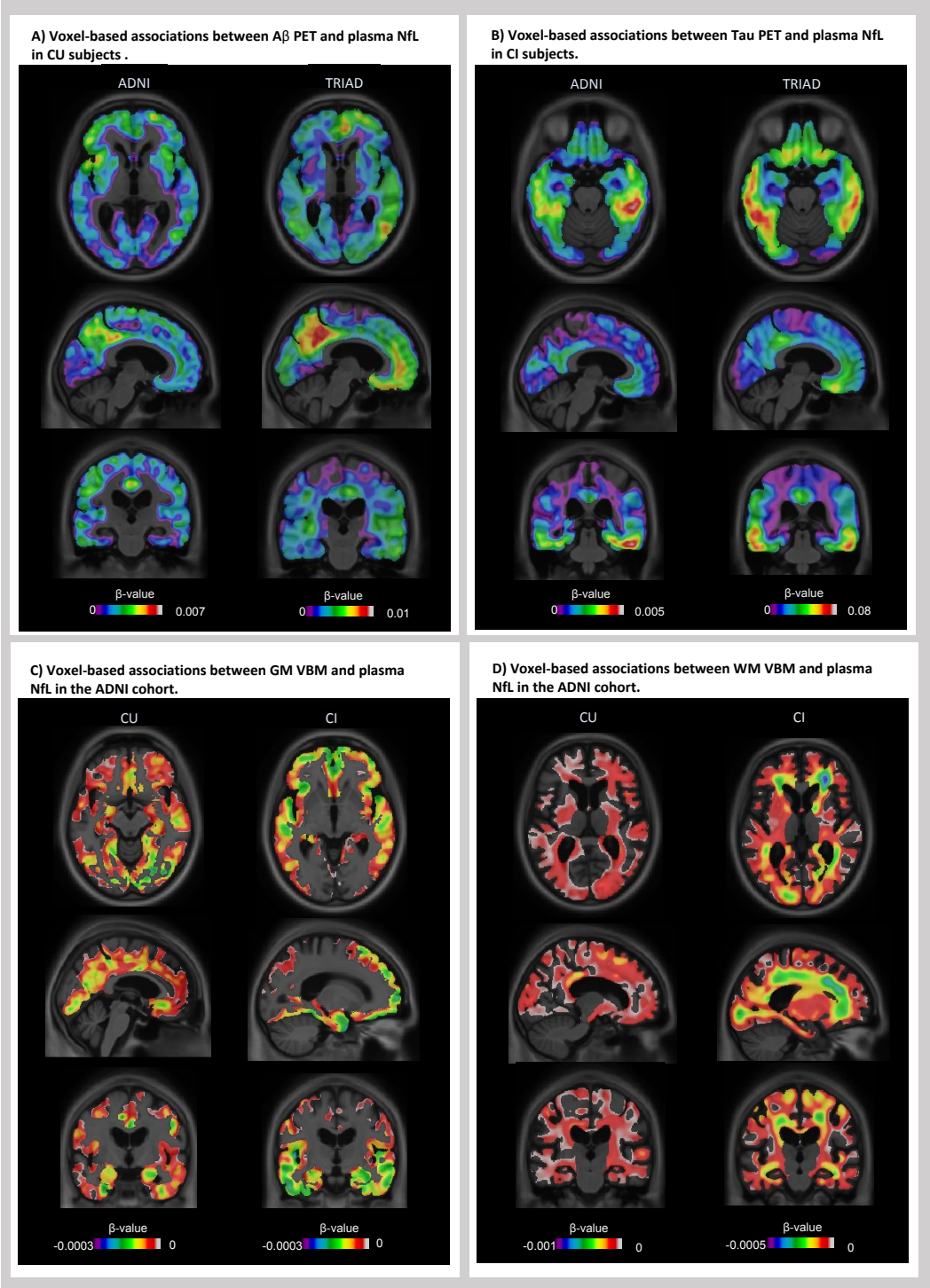

Figure S2. For each of the generalized models applied at the voxel level, ß-value maps were generated. These maps are presented here for the main findings: association between plasma NfL and Aβ PET (A), tau PET (B), GM VBM (C) and WM VBM (D).

8. Plasma NfL at baseline and longitudinally by Aβ-status

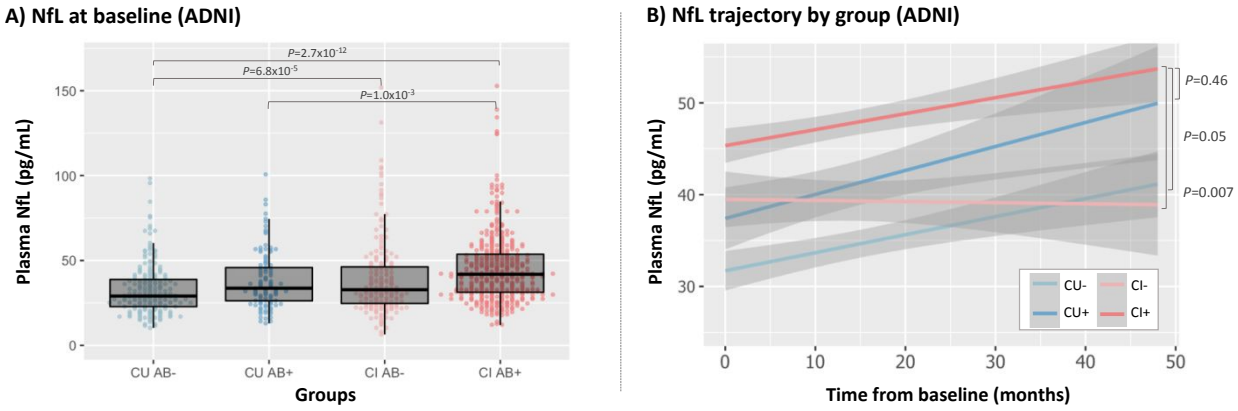

Figure S3. Plasma NfL levels at baseline (A) were significantly higher in Aβ positive CI compared to Aβ positive CU and Aβ negative CU (P<0·001). Aβ negative CI showed significantly higher plasma NfL levels compared to Aβ negative CU (P<0·001). Longitudinal trajectories for plasma NfL by Aβ status (B) showed that slopes were significantly steeper in Aβ positive CI relative to Aβ negative CI (P<0·01).

9. Associations between plasma NfL and VBM findings by Aβ-status

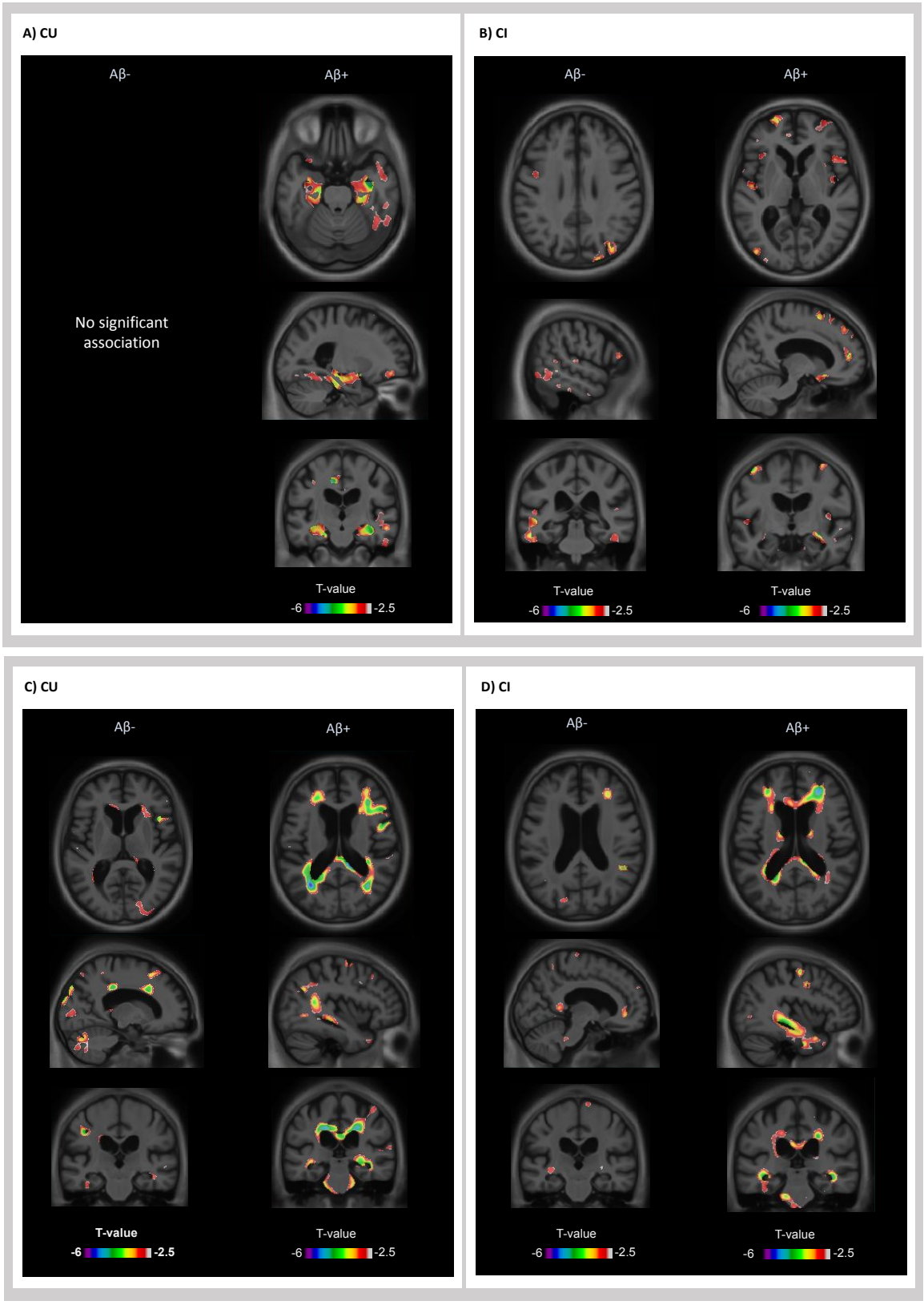

Figure S4. Associations between plasma NfL and grey matter volume are shown for CU and CI by Aβ status in panels A and B; associations between plasma NfL and white matter volume are shown in panels C and D.

STROBE Statement—checklist of items that should be included in reports of observational studies

	Item No.	Recommendation	Page No.	Relevant text from manuscript
Title and abstract	1	(*a*) Indicate the study's design with a commonly used term in the title or the abstract	3; Lines 49 and 53	
		(*b*) Provide in the abstract an informative and balanced summary of what was done and what was found	3; Lines 49-63	
Introduction				
Background/rationale	2	Explain the scientific background and rationale for the investigation being reported	Page 5	
Objectives	3	State specific objectives, including any prespecified hypotheses	Page 5; Lines 95-102	
Methods				
Study design	4	Present key elements of study design early in the paper	Page 6; Lines 106-1113	
Setting	5	Describe the setting, locations, and relevant dates, including periods of recruitment, exposure, follow-up, and data collection	Pages 6-7; appendix page 2	
Participants	6	(*a*) *Cohort study*—Give the eligibility criteria, and the sources and methods of selection of participants. Describe methods of follow-up *Case-control study*—Give the eligibility criteria, and the sources and methods of case ascertainment and control selection. Give the rationale for the choice of cases and controls *Cross-sectional study*—Give the eligibility criteria, and the sources and methods of selection of participants	Pages 6-7; appendix pages 3 and 4	
		(*b*) *Cohort study*—For matched studies, give matching criteria and number of exposed and unexposed *Case-control study*—For matched studies, give matching criteria and the number of controls per case		
Variables	7	Clearly define all outcomes, exposures, predictors, potential confounders, and effect modifiers. Give diagnostic criteria, if applicable	Pages 6-8;	
Data sources/ measurement	8*	For each variable of interest, give sources of data and details of methods of assessment (measurement). Describe comparability of assessment methods if there is more than one group	Page 8; Appendix pages 5-6	

Bias	9	Describe any efforts to address potential sources of bias	
Study size	10	Explain how the study size was arrived at	Page 6; Appendix page 3

Continued on next page

Quantitative variables	11	Explain how quantitative variables were handled in the analyses. If applicable, describe which groupings were chosen and why	Pages 8-9
Statistical methods	12	(*a*) Describe all statistical methods, including those used to control for confounding	Pages 8-9; Appendix page 7
		(*b*) Describe any methods used to examine subgroups and interactions	Pages 8-9; Appendix page 7
		(*c*) Explain how missing data were addressed	Appendix page 3
		(*d*) *Cohort study*—If applicable, explain how loss to follow-up was addressed *Case-control study*—If applicable, explain how matching of cases and controls was addressed *Cross-sectional study*—If applicable, describe analytical methods taking account of sampling strategy	Pages 8-9; Appendix page 7
		(*e*) Describe any sensitivity analyses	Not applicable
Results			
Participants	13*	(a) Report numbers of individuals at each stage of study—eg numbers potentially eligible, examined for eligibility, confirmed eligible, included in the study, completing follow-up, and analysed	Page 9; Appendix page 8
		(b) Give reasons for non-participation at each stage	
		(c) Consider use of a flow diagram	Appendix page 3
Descriptive data	14*	(a) Give characteristics of study participants (eg demographic, clinical, social) and information on exposures and potential confounders	Page 9; Table 1
		(b) Indicate number of participants with missing data for each variable of interest	Appendix page 8
		(c) *Cohort study*—Summarise follow-up time (eg, average and total amount)	Page 10; Appendix page 8
Outcome data	15*	*Cohort study*—Report numbers of outcome events or summary measures over time	Page 10; Appendix page 8
		Case-control study—Report numbers in each exposure category, or summary measures of exposure	
		Cross-sectional study—Report numbers of outcome events or summary measures	Page 9; Table 1
Main results	16	(*a*) Give unadjusted estimates and, if applicable, confounder-adjusted estimates and their precision (eg, 95% confidence interval). Make clear which confounders were adjusted for and why they were included	Pages 10-12
		(*b*) Report category boundaries when continuous variables were categorized	Not applicable

	(*c*) If relevant, consider translating estimates of relative risk into absolute risk for a meaningful time period	Not applicable

Continued on next page

Other analyses	17	Report other analyses done—eg analyses of subgroups and interactions, and sensitivity analyses	Pages 9-12
		Discussion	
Key results	18	Summarise key results with reference to study objectives	Page 12
Limitations	19	Discuss limitations of the study, taking into account sources of potential bias or imprecision. Discuss both direction and magnitude of any potential bias	Pages 12-16
Interpretation	20	Give a cautious overall interpretation of results considering objectives, limitations, multiplicity of analyses, results from similar studies, and other relevant evidence	Page 16
Generalisability	21	Discuss the generalisability (external validity) of the study results	Pages 16-17
Other information			
Funding	22	Give the source of funding and the role of the funders for the present study and, if applicable, for the original study on which the present article is based	Page 9

*Give information separately for cases and controls in case-control studies and, if applicable, for exposed and unexposed groups in cohort and cross-sectional studies.

Note: An Explanation and Elaboration article discusses each checklist item and gives methodological background and published examples of transparent reporting. The STROBE checklist is best used in conjunction with this article (freely available on the Web sites of PLoS Medicine at http://www.plosmedicine.org/, Annals of Internal Medicine at http://www.annals.org/, and Epidemiology at http://www.epidem.com/). Information on the STROBE Initiative is available at www.strobe-statement.org.